

# Further Development of the NASA X-57 Maxwell Mission Planning Tool for Mods II, III, and IV

Sydney L. Schnulo\*, Dustin L. Hall†, Jeffrey C. Chin‡, and Andrew D. Smith§

NASA Glenn Research Center, Cleveland, OH, 44135

The goal of the experimental, fully electric X-57 Maxwell aircraft is to enable lower energy consumption at cruise compared to a fuel burning baseline. A sum of subsystem benefits incorporated in the electric, airframe, and propulsion systems result in this reduction in energy consumption. The Mission Planning Tool is used to predict the performance and operation of this aircraft. It captures the aerodynamics, propulsion, heat transfer, and power system of the aircraft with trajectory optimization capabilities throughout all phases of flight. This paper details the continued development of the X-57 Mission Planning Tool and demonstrates its capability to assess the effect of subsystem performance on the integrated aircraft system. The tool can also analyze how the aircraft will react if performance goals, such as electric component efficiencies, are either not met or exceeded. The results presented achieve maximum cruise duration of the X-57 through each stage in development as well as trajectory analyses predicting component efficiency limits and energy consumption.

## Nomenclature

$A_s$	Area	$Q_{loss}$	Heat to be rejected
$Bi$	Biot Number	$P$	Power
$C_p$	Specific heat	$rpm$	Revolutions per minute
$\frac{dT}{dt}$	Rate of change in component temperature	$\rho$	Component density
$\eta$	Efficiency	$T$	Component temperature
$h$	Convective heat transfer coefficient	$T_\infty$	Ambient temperature
$I$	Electrical current	$V$	Volume
$J$	Advance Ratio	$V_{rot}$	Rotational Velocity
$k_c$	Characteristic Thermal Conductivity		
$L_c$	Characteristic length		

## I. Introduction

The X-57 Maxwell is NASA's experimental fully electric aircraft and is shown in Figure 1. The goal of the X-57 program is to use distributed electric propulsion to enable a five times reduction in energy consumption at cruise compared to the baseline Tecnam P2006T.<sup>1</sup> There are three ways in which this reduction in energy will be achieved: a fully electric architecture, wingtip cruise propulsion, and a high aspect ratio wing enabled by distributed electric propulsion. The aircraft will be powered by batteries that drive electric motors connected to the propellers. Each of these components have an efficiency of at least 95 percent. This results in an energy transmission efficiency from battery to propulsor upwards of 90 percent. This proves to be a large advantage compared to diesel fuel engines, which tend to operate at 37 percent efficiency, and gas turbine engines that are closer to 15 percent efficiency at this size class.<sup>2</sup> This electric architecture also allows propulsion airframe integration that would not be possible with mechanical shafting.

\*Aerospace Engineer, Propulsion Systems Analysis Branch, sydney.l.schnulo@nasa.gov, and AIAA Member.

†Aerospace Engineer, Propulsion Systems Analysis Branch, dustin.l.hall@nasa.gov, and AIAA Member.

‡Aerospace Engineer, Propulsion Systems Analysis Branch, jeffrey.c.chin@nasa.gov, and AIAA Member.

§Aerospace Engineer, Thermal Systems and Transport Processes Branch, andrew.d.smith-1@nasa.gov, and AIAA Member.



Figure 1: NASA’s Scalable Convergent Electric Propulsion Technology Operations Research (SCEPTOR) final Mod IV fully electric X-57 aircraft concept with distributed propulsion.

The wingtip propellers rotate to counteract the wingtip vortices to achieve a second source of benefit. The high aspect ratio wing of the aircraft results in a three times reduction in wing area, and therefore drag. The six smaller high lift propulsors on each wing enable this decrease in area by augmenting lift at takeoff and landing. The high lift propellers then fold back at cruise to remain aerodynamic and the propulsion comes solely from the cruise motors on the wingtips.

The energy savings of this aircraft result from the interaction of the electric, the propulsion, and aerodynamic systems. The Mission Planning Tool (MPT) is used to assess the performance of these subsystems in context of the whole aircraft. The MPT utilizes trajectory optimization to model the behavior of the X-57. This paper focuses on the development and uses for the Mission Planning Tool through its three modifications. The cruise duration of X-57 is maximized to demonstrate the capabilities of the MPT. Cruise duration is maximized because the X-57 relies heavily on battery technology and, at this time, state of the art batteries have 4 percent of the energy density of fuel.<sup>2</sup> This energy density affects the duration of flight. Trades in component performance and an analysis of energy consumption will also be performed and presented in this paper. The Mission Planning Tool is an effective way to analyze and inform the design of the X-57 to model its behavior in flight.

### A. Stages of X-57 Maxwell Development

The aircraft is being developed in a series of four modifications, or Mods. The Mission Planning Tool has models to represent the architecture of the different Mods. The first modification is the baseline aircraft, the Tecnam P2006T. This is a conventional fuel burning aircraft with two Rotax engines that was instrumented and flown to collect data as the baseline for performance comparison.<sup>3</sup> In the second modification, Mod II, the baseline Tecnam airframe is outfitted with a fully electric configuration. This modification, shown in Figure 2a, replaces the rotax engines with batteries in the fuselage and a 72 kW permanent magnet motors on each wing. Mod II includes the development and testing of the battery and electric system.

Mod III incorporates the high aspect ratio wing and wingtip propulsion. Here the original Tecnam wing is replaced with the smaller wing that has weighted pods on it to represent the high lift motors with propellers in their folded configuration. The cruise motors are also moved outboard to the wingtips. Mod III is shown in Figure 2b. The high lift propulsors are added in Mod IV, which will test the fully distributed propulsion system and the ability to augment lift at takeoff and landing in order to lower the stall speed of the aircraft. Mod IV is the final aircraft configuration and is shown in Figure 1.

### B. Previous Work

This paper builds on two key previous works. In the first study, Falck, et al., demonstrated that trajectory optimization allows the imposition of thermal constraints to inform the flight path.<sup>4</sup> The Mission Planning



(a) X-57 Maxwell Mod II with original Tecnam wing and electric motors. (b) X-57 Maxwell Mod III with smaller wing, wingtip electric motors, and weighted high lift motor pods.

Figure 2: First two electrified modifications of the X-57 Maxwell, Mods II and III.

Tool includes many of the models and methodologies presented in Falck’s paper. In the other key previous work, we showed that by using trajectory optimization through optimal control methods we were able to model a mission that uses 32 percent less energy than a simple baseline trajectory.<sup>5</sup> This paper also details the methods used to model all phases of flight: taxi, motor run-up, takeoff, climb, cruise and descent. Both of these works, as well as the current MPT, use a tool called Dymos, which is a trajectory optimization tool that implements pseudospectral optimal control methods.<sup>6</sup> Dymos is written using the OpenMDAO framework, an open source multidisciplinary design, analysis, and optimization software written in python.<sup>7,8</sup> These two studies detail many of the models used in the Mission Planning Tool.

Two other previous works are used heavily in the Mission Planning Tool to build subsystem models. Chin, et al, presented the characterization of the Samsung 18650 cells that provided performance maps to be used in Thevenin circuit battery model for the Mission Planning Tool.<sup>9,10</sup> This provided performance maps of specific battery cells being used for X-57 with respect to state of charge and temperature. Borer’s studies provide the aerodynamics for this paper, as well as models for the propulsion airframe interaction.<sup>11</sup> These studies provide pivotal performance information of the battery and aerodynamic subsystems for integration into the Mission Planning Tool.

### C. Assumptions

The results presented in this paper have key component and mission assumptions. The component assumptions refer to the efficiency and temperature limits of the electric components, while mission assumptions affect the phases of flight. Note that these efficiency assumptions will be refined as component hardware is delivered and tested, which will be essential in predicting the flight of the aircraft. This is because a change in efficiency will affect the heat load of the electric components, as well as the power required from the battery. Table 1 lists the electric system technology assumptions.

Table 1: Electric system temperature limit and efficiency assumptions.

Component	Temperature Limit, $K$	Peak Efficiency, %
Cruise Motor	373	96
Cruise Motor Controller	423	97
High Lift Motor	423	93
High Lift Motor Controller	373	98
Power Bus	353	99.6*
Battery	353	98**

\* Wire efficiency is length dependent.

\*\* Cell level resistance is determined in performance maps as a function of SOC and temperature. 98 percent refers to pack level losses.

The phases for the assumed mission are shown in table 2. The amount of time for a phase is listed in seconds and altitude is listed in feet above the Mean Sea Level (MSL). 2372 ft reflects ground level at Edwards Air Force Base. Velocity is shown in knots calibrated airspeed. If the time is not listed for a phase,

Table 2: Mission assumptions for all modifications.

Phase	Time, s	Altitude, ft MSL	Calibrated Airspeed, kn
Taxi	300	2372	24
Motor Check	30	2372	0
Takeoff	–	2372	0 to $V_{rot}$
Climb	–	2372 to 6000	$V_{rot}$ to 120
Cruise	–	6000	120
Descent	–	6000 to 2372	120 to $V_{rot}$

it signifies that time is a design variable in the optimization. This occurs in takeoff, climb, and cruise. In takeoff, time is determined by how long it takes to reach the rotational velocity of the aircraft with motors at full throttle. For climb and descent, each modification will have an optimal climb speed that uses the least energy. Finally, because in this paper the objective is to maximize cruise duration and range, cruise time also becomes a design variable.

Additionally, the aircraft weight goal across all Mods is 3000 lbs. The batteries are assumed to start at a state of charge of 95 percent and the max discharge capacity is 20 percent for battery health purposes. The 20 percent margin also can act as a reserve for higher duration operations. Finally, the cruise motors are torque controlled, with a speed of 2250 rpm for the cruise motors. All of the analyses presented in this paper include these assumptions.

## II. Mod II Tool Development

The continued development of the Mission Planning Tool is essential in ensuring an accurate simulation of flight. Although previous work included the development of MPT for Mod II,<sup>5</sup> subsystem models mature as components are tested, which result in a more accurate tool. For the Mod II analysis, two specific models that have been added to the tool since the original optimization are the installed drag penalty for the propeller and the battery performance maps mentioned in the previous section.<sup>9</sup>

### A. Installed Drag Penalty

The effect of installed drag of the Mod II propellers is added into the overall aircraft model. The propellers' thrust penalty due to installation on the airframe is modeled as a correction factor on the propeller efficiency. The correction factor, shown in Equation 1, is derived from empirical data from the Mod I flight.

$$\eta_{corrected} = \eta_{base}(J, rpm) + \eta_{base}(J, rpm) * 0.0371 * J - 0.1515 \quad (1)$$

In this equation,  $\eta_{corrected}$  is the propeller efficiency with the empirical installed drag factor applied,  $\eta_{base}(J, rpm)$  is the value of efficiency given by the propeller performance map as a function of  $J$ , the advance ratio, and  $rpm$ . The installed propeller correction factor raises the shaft power requirement of the aircraft at cruise from 48.4 kW to 54.2 kW, so by about 12 percent.

## B. Mod II Maximum Cruise Duration Analysis

Cruise duration is an important parameter to maximize because this is where flight data is collected for comparison to the baseline. The maximization of cruise duration translates to the maximization of cruise range because the airspeed and altitude are constant at this phase of flight. To complete this analysis, the objective of the optimization is to maximize cruise time with a required 20 percent minimum state of charge at landing. Constraints are also in place to ensure that component temperatures stay within their limits. The results of this optimization for the nominal mission is shown in Figure 3.

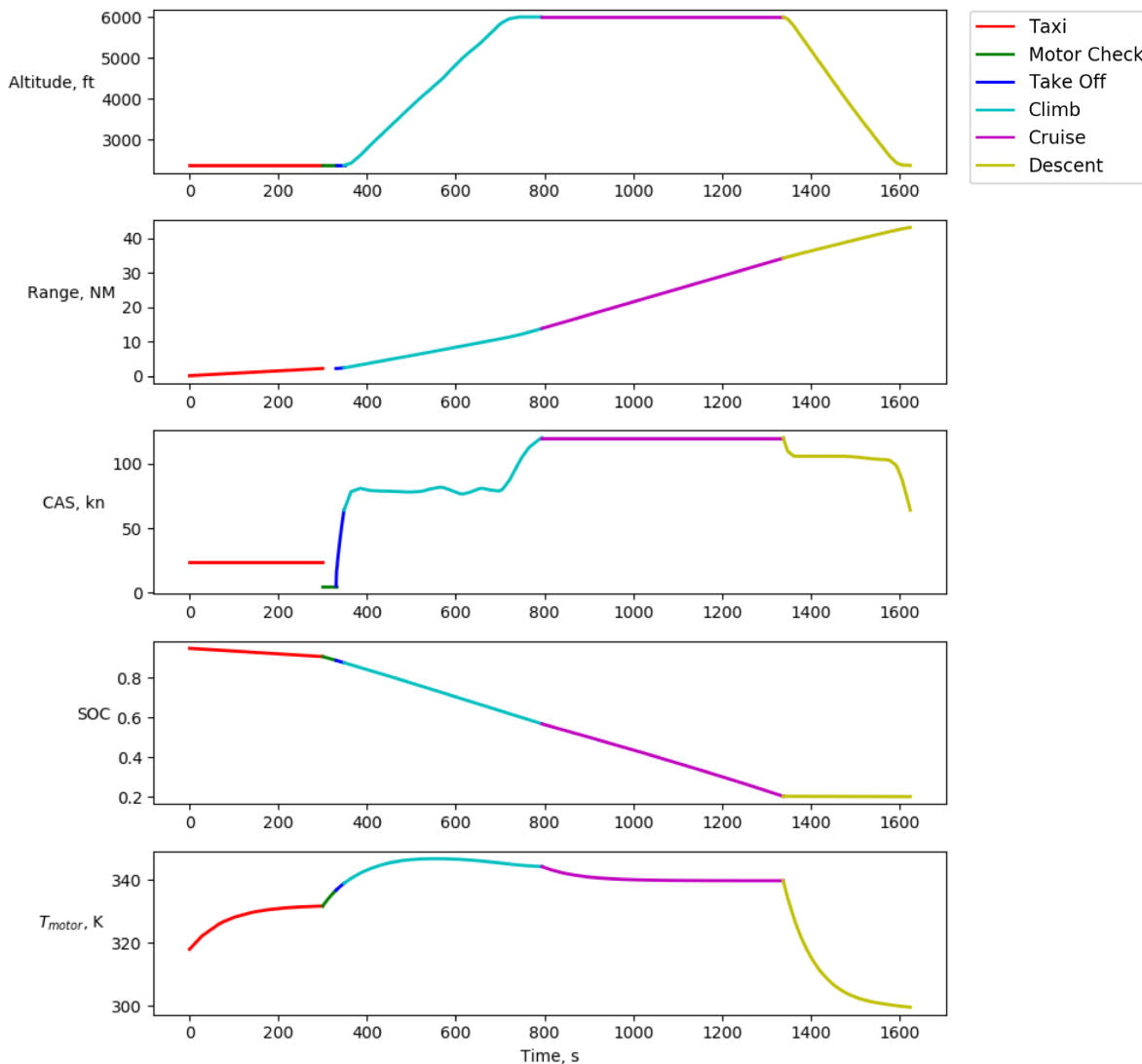


Figure 3: Mod II mission optimized for maximum cruise duration gives a cruise time of 9 minutes and 3.5 seconds for 20.4 NM of range.

This objective causes the aircraft to minimize the energy spent at takeoff, climb, and descent so that it uses the most at cruise. Taxi and motor check phases are fixed, and for takeoff it accelerates at maximum power until it reaches 64 kn. There is an optimal climb rate of 590 ft/min at 80 NM. After leveling out at 6000 ft, the aircraft cruises for a little over 9 minutes for a maximum cruise range of 20.4 NM at a

calibrated airspeed of 120 kn. Then the aircraft descends for 4 minutes, 45 seconds at a just over 100 knots before decelerating back to 64 kn for landing. The component temperatures stay within their limits with a maximum cruise motor temperature of 347 K during climb.

### C. Efficiency Trades

Hardware testing of the cruise motors show that they are reaching temperature limits faster than was originally thought. Analysis of the motor configuration and data suggest that the motor efficiency could be lower than was originally predicted and referred to in this assumptions section.<sup>12</sup> The Mission Planning Tool is used to assess the effect that this will have on the mission. For this study, a range of efficiency values of the motor are applied to optimizations of the maximum cruise duration, which effect range and cruise time. Constraints on this optimization include a 20 percent final SOC to coincide with our nominal mission, and a maximum motor temperature of 373 K. The results are shown below in Figure 4.

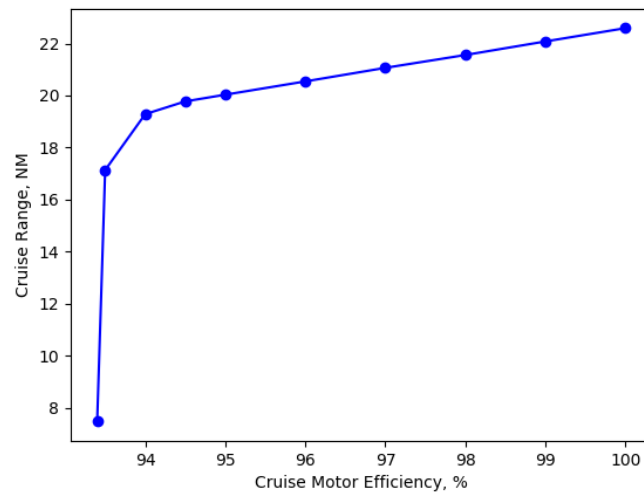


Figure 4: Motor efficiency sweep study showing the maximum cruise range of the aircraft at 6000 ft, 120 KCAS.

The study shows that above 95 percent motor efficiency, there is a linear trend in which a one percent increase in efficiency enables approximately an additional 0.5 NM of range. This means that a 100 percent efficient motor would increase cruise range by 2 NM. This is due to the fact that higher motor efficiency will require less power draw from the battery to provide the same propeller shaft power, and therefore thrust. Below 95 percent the range decreases more dramatically with small changes in efficiency. Because of the higher heat load, the motor reaches its temperature limit in these instances, so the aircraft climb rate decreases. Figure 5 displays a closer look at the aircraft trajectories at different cruise motor efficiency values.

At 94 percent efficiency and below, climb rate decreases because the motor must use less power (and produce less heat) to stay within its temperature constraints. It also takes longer to accelerate to its cruise speed of 120 kn for the same reason. However, overall this climb uses more energy because the time to climb to altitude is higher, forcing a reduction in the cruise duration. At 93.5 percent motor efficiency, the cruise motor temperature remains at the temperature limit over cruise. If the efficiency goes lower, then the cruise motor will overheat during cruise causing cruise duration to reduce further.

This translates to critical information for mission planning. If final component testing shows that the cruise motor has less than 95 percent efficiency, either the design or operation of the aircraft must change. The design approach would be to modify the thermal management system to provide higher heat dissipation capabilities. The Mission Planning Tool can inform the heat transfer coefficient required of a new thermal management design. Operationally, the pilot must climb at a slower rate to avoid overheating the motors, resulting in a reduction in cruise time. The Mission Planning Tool can be used to assess these alternatives,

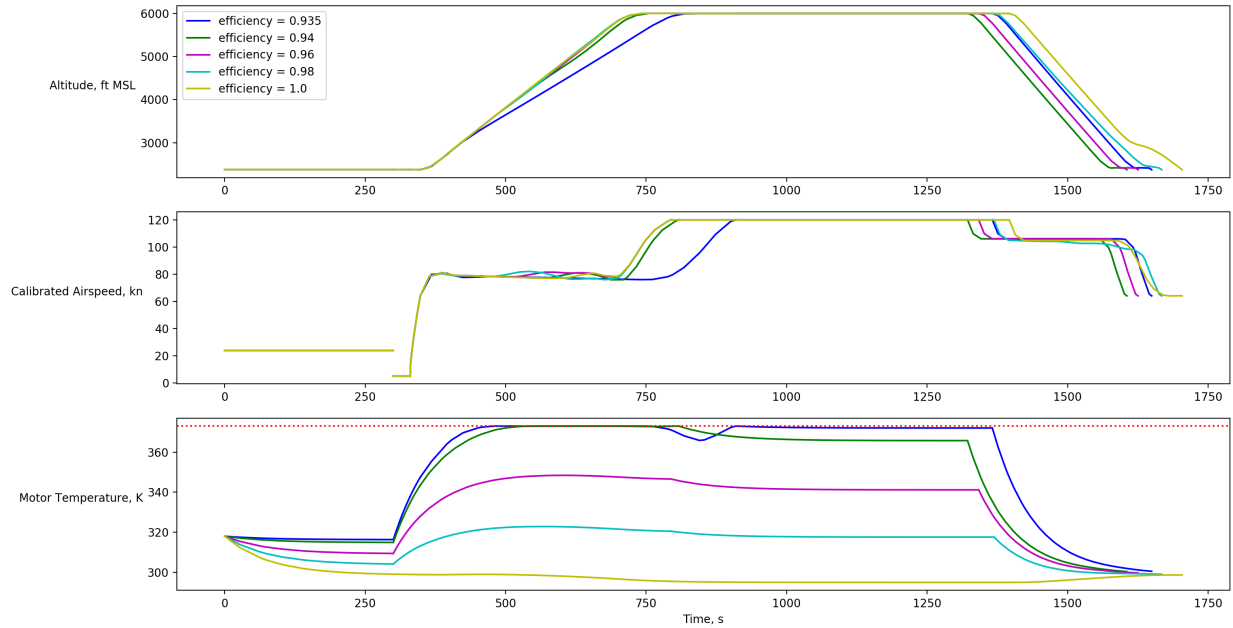


Figure 5: Trajectory details for motor efficiency sweep given the objective of maximum cruise duration. The dotted red line indicates the maximum motor temperature.

and help identify where these limits lie. As more of the X-57 components are tested to verify performance numbers, the tool will be used to assess solution options.

### III. Mod III Tool Development

As discussed in the Introduction, the Mod III stage replaces the original Tecnam wing with the high aspect ratio wing. The Mod III version adds models to the Mod II tool to reflect both the smaller wing and the wingtip propulsion. The first adjustment involves changing the wing area and computing the drag associated with the smaller area. The second adjustment is in the length of the cabling, which affects the power loss. Finally, the third change accounts for the aerodynamic effect of the wingtip propulsors, which counteract the wingtip vortices. This will reflect the energy savings in Mod IV.

#### A. Modeling Wing Area Reduction and Wingtip Propulsion

Drag is found using Equation 2 to capture the new wing and propulsor configuration for Mod III.

$$D = S * C_D \quad (2)$$

$D$  refers to drag,  $S$  is reference wing area, and  $C_D$  is the coefficient of drag. In Mod III and Mod IV, the reference area is 67 square feet as opposed to 159 square feet for Mod II, which will therefore decrease drag by the same factor. The next feature of Mod III that needs to be captured is the relocation of the cruise motors to the wingtips. There are two steps in modeling this. The first step is capturing the effect of the longer power bus on the power system. Essentially, this results in more heat loss due to resistance, as seen in Equation 3

$$Q = I^2 * R * L \quad (3)$$

where  $Q$  is heat, or power loss from the wire,  $R$  is the resistance per length of the copper power bus, and  $L$  is the length of the bus. In Mod III, this length roughly triples compared to Mod II. Luckily, this length increase also provides more thermal mass, so the thermal performance remains constant. It does, however, reduce the electric transmission efficiency from the battery to the motor shaft to 92.7 percent compared to 93.2 percent in Mod II. The second step in modeling the wingtip cruise motors is capturing the effect of the

propellers rotation counteracting the wingtip vortices. This becomes a “negative drag” in the equations of motion. The value is provided in the aerodynamics data as a function of altitude and true air speed.<sup>11</sup>

## B. Mod III Maximum Cruise Duration Analysis

The maximum range optimization is repeated for the Mod III configuration. To do this, the major adjustment is that the rotational velocity of the aircraft is 88 knots rather than 64 knots to account for the higher aircraft stall speed. The results are shown in Figure 6. Because of the higher stall speed, the duration of the takeoff

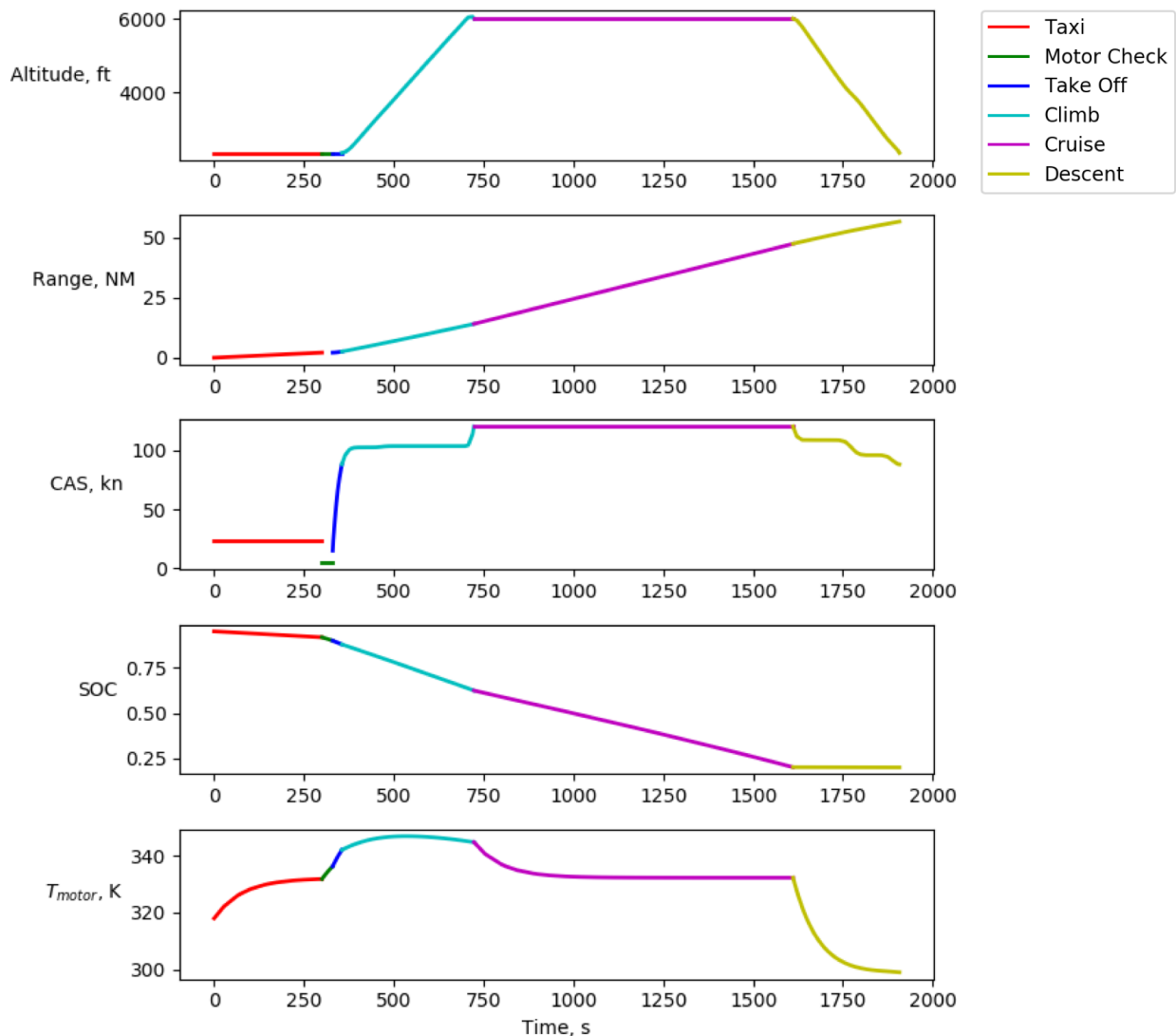


Figure 6: The maximum cruise range of the Mod III vehicle is 33.3 nautical miles with the nominal mission.

phase is 25 seconds, compared to 18 seconds in Mod II. A longer time at takeoff may raise concern for the temperature of the cruise motor, but the results show that the temperature actually begins to fall as airspeed continues to increase, providing more cooling. In Mod IV, takeoff duration will be reduced with the additional thrust and lift from the high lift motors. The climb phase takes just over six minutes. It occurs at a calibrated airspeed of 103 kn and a climb rate of approximately 630 ft/min. The cruise segment then lasts for 14 minutes and 50 seconds for a total cruise range of 33.3 NM. The aircraft then descends for 5 minutes using minimal energy. The increase in cruise time over Mod II reflects the energy savings of the Mod III configuration, which will be considered in more detail in the next section.

### C. Energy Usage at Cruise

The Mission Planning Tool can be used for simpler studies without running a full trajectory optimization, as will be demonstrated in this section. As stated in the Introduction section, one of the goals of the X-57 Maxwell program is to show a energy reduction at cruise. These energy savings are to be demonstrated in the Mod III vehicle, with benefit coming from the fully electric architecture, the reduction in wing area, and the wingtip propulsion. The Mission Planning Tool can predict the total benefit seen from these three changes in architecture over the baseline. Cruise phase analyses are ran for steady level flight at the nominal cruise condition: 120 kn at 6000 ft. The Mod II results show that it requires a shaft power of 54.2 kW at this flight condition. Mod III gives a required shaft power of 39.6 kW. By simply switching to the smaller airfoil and wingtip propulsion, there is already a shaft power savings of 27 percent. Because the Mod II aircraft uses the same wing and airframe as the fuel burning Mod I baseline, the shaft power required for Mod I is also 54.2 kW. Equation 4 yields energy consumption.

$$P_{source} = \frac{P_{shaft}}{\eta} \quad (4)$$

In this equation,  $P_{shaft}$  refers to the shaft power required and  $\eta$  is the efficiency of the transmission from the source. This transmission will be mechanical in Mod I and electrical in Mods II and III. In Mod I, the efficiency of a state-of-the-art diesel engine is assumed to be 37 percent.<sup>2</sup> Therefore, the results of the study are shown below.

Table 3: Energy savings study for electric X-57 Modifications.

	Mod I	Mod II	Mod III/IV
$P_{shaft}, kW$	54.2	54.2	39.6
$\eta$	0.370	0.932	0.927
$P_{source}, kW$	146.5	58.2	42.7

At this flight condition, Mod I is predicted to use 2.5 times more energy than Mod II and 3.4 times more energy than Mod III. This study does not consider the lapse in efficiency with altitude for the diesel engine, which does not occur in an electric system. Therefore, this is a conservative estimate of the performance of the electric aircraft over the baseline in terms of energy consumption.

## IV. Mod IV Tool Development

The Mod IV version of the Mission Planning Tool captures the effects of the high lift propulsion system. This includes the models that were added for Mod III, but also the aerodynamic effects of the high lift motors as well as their additional power draw required for the Mod IV tools.

### A. High Lift Motor System

In Mod IV, the high lift propulsors are added to the Mod III aircraft. Analysis outputs a performance table outputs the power required at the high lift motor shaft and coefficient of drag as a function of altitude and airspeed. This data comes from detailed analyses done in Xrotor and CFD to capture the propulsion airframe interactions occurring while the wing is being blown.<sup>11</sup> This coefficient of drag adder is a negative value, simulating a reduction in drag and therefore a higher lift-to-drag ratio than would result from an unblown wing. The electric system model must be updated to include the high lift motor system.

#### 1. Electric System Architecture

The electric system in Mod IV has a different architecture than Mods II and III. This is to account for the high lift motor system. On each wing, there are two parallel modeling paths for power to flow from the battery, as can be seen in Figure 7. MPT models one half of the electric system and then multiplies it by two to reflect the whole aircraft. Like in Mods II and III, the cruise propeller gives the shaft power required

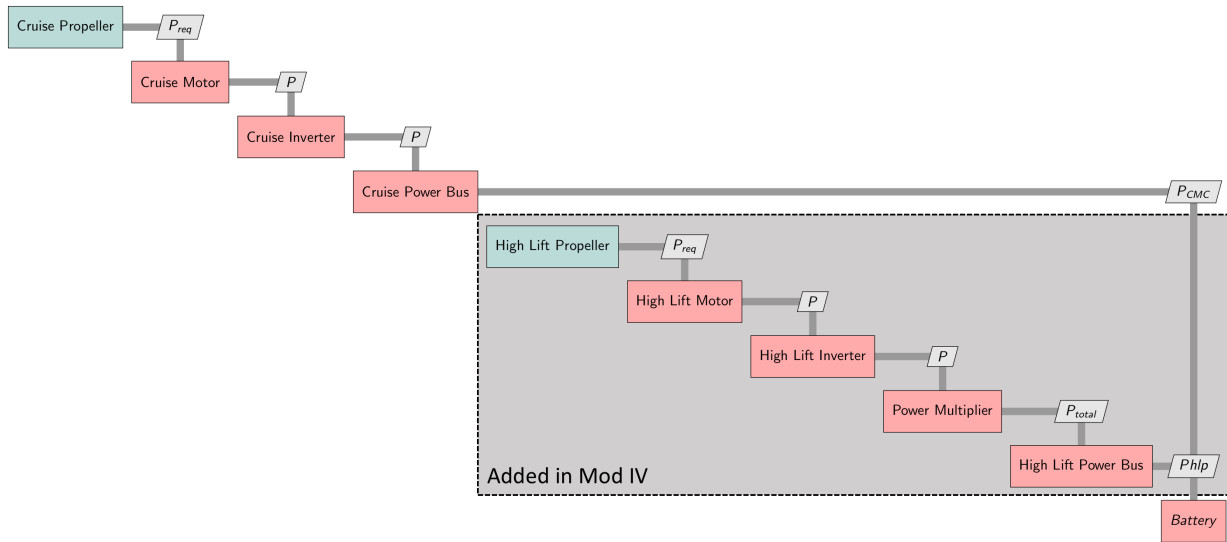


Figure 7: One half of the electric system architecture for the Mod IV configuration.

at the output. The cruise motor then uses this value to determine the power required at its input given its efficiency. The model repeats this for the cruise motor inverter and the cruise power bus to give the output of cruise power required from the battery.

For Mod IV, there is a parallel power bus that supplies power to the high lift inverters. This is done in much the same way as for the cruise system. The shaft power required for one cruise propeller is supplied as an input to the system and this is fed through the high lift motor and inverter. A Power Multiplier component multiplies the power required by each inverter by six to represent the whole array of high lift motors. This value passes through the high lift power bus, where losses between each motor are neglected at this time. The power required by the high lift system plus the power required by the cruise motors yields the power demanded from the battery.

The high lift motors are only active at takeoff, initial climb, and landing to augment lift. Therefore, at all other times in the mission the power required to the high lift system is zero. All phases of flight include the high lift system so that component temperatures can be tracked.

## 2. High Lift Propulsor Thermal Modeling

The design of the high lift propulsors is important for the operation of the X-57 Maxwell in takeoff and landing. The 14 kW inverters have been designed for thermal management through outer mold line cooling, meaning that there is a conductive heat sink path to the nacelle surface, where heat is lost to convection. This thermal management solution is advantageous because passive cooling does not add any drag, unlike the more complicated cooling architecture of the higher power cruise motors.<sup>13</sup> The transient analysis of the motor and inverter rely on a lumped capacitance heat transfer model. At this time, the high lift motor design has not been chosen, but the high lift inverter has been fully designed and tested. For integration into the Mission Planning Tool, the goal of this analysis is to determine the junction temperature in the high lift inverters in order to ensure that the MOSFETs will not overheat in any condition. Because the heat sink and the thermal film have high values of thermal diffusivity,  $6.90 \times 10^{-5} \text{ m}^2/\text{s}$  and  $6.58 \times 10^{-5} \text{ m}^2/\text{s}$  respectively, the energy is dissipated much faster than it can be stored. Because of this, the lumped capacitance method may be used. To determine the validity of using the lumped capacitance method, the Biot number of the heat sink is calculated for the system. The Biot number determines the ratio of the conductive and convection heat dissipation, as seen in Equation 5.

$$Bi = \frac{h * L_c}{k_c} \quad (5)$$

$L_c$  is the characteristic length calculated as the volume of the heat sink divided by the external surface area and  $k_c$  is the characteristic thermal conductivity of the system. To calculate the characteristic thermal conductivity, the thickness of each material between the junction and the convection path is multiplied by its respective thermal conductivity before being normalized by the total thickness. Table 4 below lists the values used in this process.

Table 4: Values to determine characteristic thermal conductivity ( $k_c$ ).

Component	Thickness, mm	Normalized Thickness	Thermal Conductivity, W/mK
Chip Wall	0.0500	0.0065	2.2
Thermal Film	0.0254	0.0030	5.0
Heat Sink	7.6200	0.9902	167.0

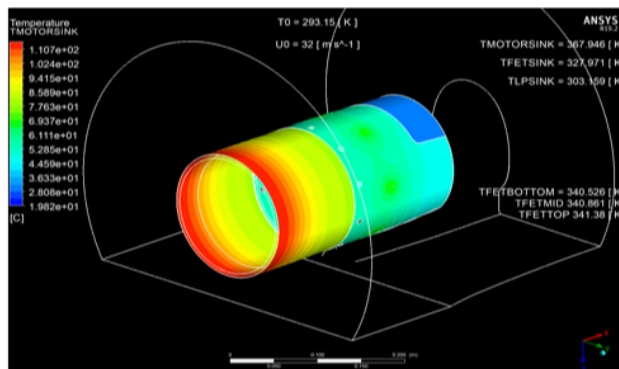
The Biot number is 0.001, indicating that the error associated with using the lumped capacitance method is small.<sup>14</sup>

An energy balance of the surface can be conducted to relate the rate of energy out of the system with the rate of change of internal energy within the system. Heat is only dissipated through convection. Equation 6 relates Newton's law of cooling to the rate of change in internal energy at the surface.

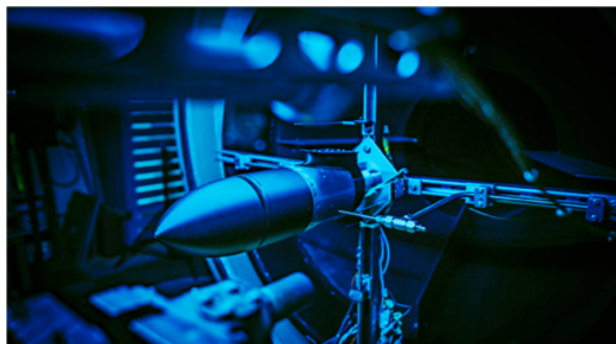
$$Q_{loss} - hA_s(T - T_\infty) = \rho VC_p \frac{dT}{dt} \quad (6)$$

The temperature rate of change ( $\frac{dT}{dt}$ ) is then used by Dymos for the integration of the temperature state of the component throughout the mission. The same approach is taken for the other electric components, with heat capacity values for the high lift motor pending a decision on motor design.

High fidelity analyses and testing were done to characterize the convection heat transfer coefficient for both the motor and the generator. First, an ANSYS thermal analysis was completed that approximates the high lift nacelle as a cylinder with heat loads applied to the forward and aft segments to simulate the motor and converter, respectively. This is shown in Figure 8a.



(a) High left motor nacelle simulation in ANSYS.



(b) High lift propulsor thermal test setup

Figure 8: Analyses and testing to characterize the convection coefficient at the high lift propulsors.

Figure 8b depicts the testing done to verify the high fidelity analyses. Here, a replica of the nacelle was outfitted with thermocouples and placed in a small wind tunnel. Heat loads were applied and data collected that corroborated the analyses. The results of heat transfer coefficient as a function of airspeed are presented in Figure 9.

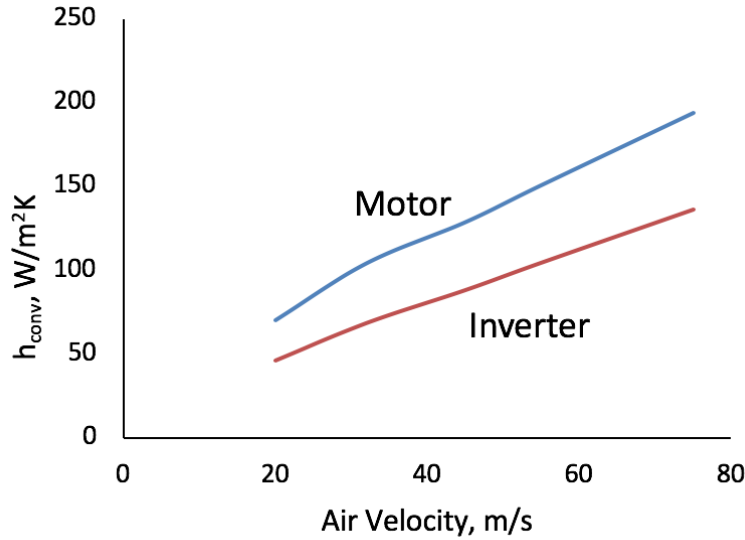


Figure 9: Results of high lift propulsor thermal analyses and testing gives the convection coefficient as a function of air velocity.

These trends yield linear equations for convection coefficients. The motor convection coefficient is assumed to be

$$h_{motor} = 2.199 * v_{cool} + 29.972 \quad (7)$$

and the convection coefficient at the inverter is found using

$$h_{inverter} = 1.619 * v_{cool} + 15.407 \quad (8)$$

While the high lift motor controller has been fully designed and tested, the design for the high lift motor has not. Therefore, conservative values of efficiency and heat capacity are assumed and may not reflect the final motor configuration. This should also be remembered as the mission analyses are performed. However, this thermal characterization is useful in informing the design.

## B. Mod IV Maximum Cruise Duration Analysis Results

The addition of the high lift propulsion system results in two new phases of flight: high lift motor check and high lift propulsor climb. First, a phase is added to test the high lift motors. In this phase, only the high lift propulsors are run at full power for 30 seconds. Next, the tool models climb differently for Mod IV. The Mod II and Mod III versions modeled climb and descent as one phase. Mod IV breaks climb into a high lift propulsor (HLP) climb and climb. The operation of the high lift motors augments lift in the HLP climb phase. In climb, the tool still tracks the temperatures of the high lift motors, but the motors are at zero power. The Mod IV mission optimization includes these phase additions.

The objective of the optimization remains consistent with Mods II and III: maximize cruise duration. The results of the climb optimization are given in Figure 10. The results show that takeoff duration is reduced to 11 seconds with the high lift motor thrust and lift. The aircraft climbs at 68 knots with the high lift motors operating until an altitude of 3990 feet. The initial climb phase lasts for 1 minute and 46.7 seconds. Airspeed in the climb phase increases to 103 knots when the high lift motors are powered down and the propellers are folded back This is consistent with the Mod III vehicle climb speed. The aircraft climbs to altitude in 5 minutes and 30 seconds, resulting in an end of climb state of charge of 61.4 percent. The end of climb state of charge in Mod III is 62.4 percent, while staying within temperature limits for the cruise motor (CM), high lift motor controller (HLMC), and all other electric components. This suggests that although there is more power being used for takeoff and climb in order to operate the high lift motors, a reduction in the duration of these segments results in comparable energy usage. The results show a maximum cruise

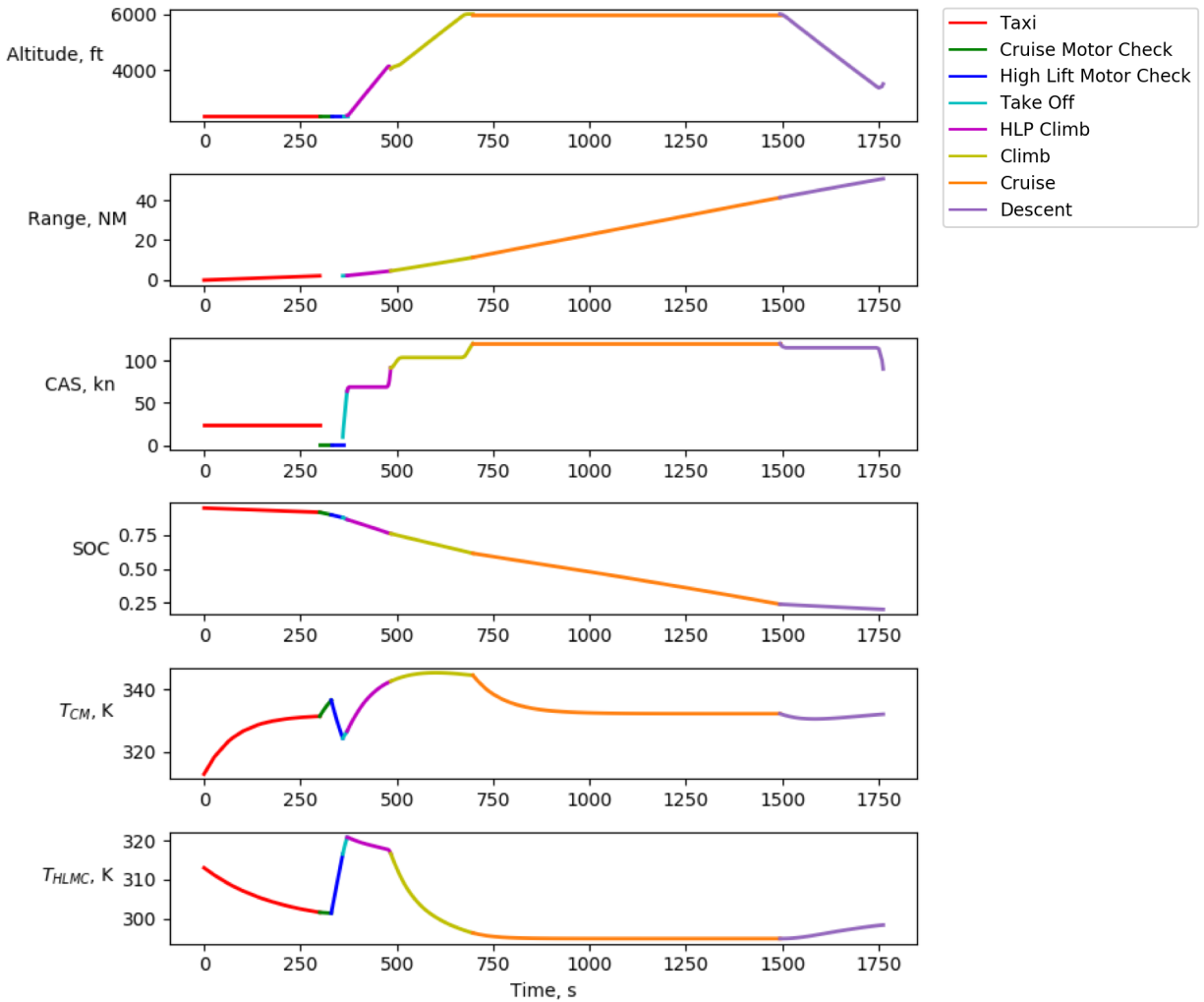


Figure 10: Results of Mod IV cruise range optimization.

range of 29.8 NM in 13 minutes and 17 seconds. The aircraft then descends at minimal power draw. The final approach phase of this analysis is not modeled, as there are many ways to operate the high lift motor system at landing that are still being considered.<sup>15</sup> Overall, the Mod IV results yield a takeoff field length that is less than that of Mod II and a low energy consumption at cruise. This aligns with the programs goals.

## V. Conclusions and Future Work

The Mission Planning Tool is a versatile resource to model the performance of the X-57 Maxwell at an aircraft level. By using the Mission Planning Tool, the subsystem designs can be evaluated in context of operation of the aircraft to mitigate risks. The tool has been developed to model all phases of flight for Mods II, III, and IV of the X-57 program. These analyses found that in Mod II, the motor efficiency is critical to the cruise range of the aircraft. Using nominal mission assumptions, an efficiency less than 95 percent causes concern for the motor overheating in climb. In Mod III, the Mission Planning Tool showed that the aerodynamic benefits of the X-57 show a 25 percent reduction in power at the nominal cruise condition, and adding the electric architecture resulted in 3.5 times less energy consumption over a the fuel burning baseline. Finally, in Mod IV, a new electric system model for the high lift motor system and its thermal properties reflected the fully distributed propulsion. A maximum range cruise analysis predicted that the design can achieve program goals.

There are plans to continue improvements on the Mission Planning Tool as the subsystem models improve and testing data becomes available. One improvement is to integrate the aerodynamic analysis into the tool rather than using tables that are previously generated. As testing occurs, the model will be updated accordingly to represent the aircraft as closely as possible. Finally, the implementation of the Dymos tool will improve in a way that well conditions the problem from the start will reduce computational cost by automatically scaling the problem. Overall, it has been demonstrated that this tool can be used as a way to perform trade studies, optimize the trajectory, and inform subsystem designs. The Mission Planning Tool will continue to support the X-57 team in design and test planning as it moves through its stages of development.

## Acknowledgments

The authors would like to acknowledge the Flight Demonstration Capabilities (FDC) as well as the Transformative Tools and Technologies (TTT) project for funding this work. We would also like to thank Nicholas Borer, Robert Falck, and Justin Gray for their guidance and support in the development of the Mission Planning Tool.

## References

- <sup>1</sup>Borer, N. K., Patterson, M. D., Viken, J. K., Moore, M. D., Bevirt, J., Stoll, A. M., and Gibson, A. R., "Design and Performance of the NASA SCEPTOR Distributed Electric Propulsion Flight Demonstrator," *16th AIAA Aviation Technology, Integration, and Operations Conference*, No. AIAA 2016-3920 in AIAA Aviation, American Institute of Aeronautics and Astronautics, June 2016.
- <sup>2</sup>Snyder, C., "Design and Development of a 200-kW Turbo-electric Distributed Propulsion Testbed," No. 2016-461 in Propulsion Energy, American Institute of Aeronautics and Astronautics.
- <sup>3</sup>Nicolosi, F. and De Marco, A., "Stability, Flying Qualities and Parameter Estimation of a Twin-Engine CS-23/FAR 23 Certified Light Aircraft," No. 2010-7947, August 2010.
- <sup>4</sup>Falck, R., Chin, J., Schnulo, S., Burt, J., and Gray, J., "Trajectory Optimization of Electric Aircraft Subject to Subsystem Thermal Constraints," *18th AIAA Aviation Technology, Integration, and Operations Conference*, No. 2017-4002 in AIAA Aviation, American Institute of Aeronautics and Astronautics, June 2017.
- <sup>5</sup>Schnulo, S., Chin, J., Smith, A., Falck, R., Gray, J., Papathakis, K., Clarke, S., Reid, N., and Borer, N., "Development of a Multi-Phase Mission Planning Tool for NASA X-57 Maxwell," *18th AIAA Aviation Technology, Integration, and Operations Conference*, American Institute of Aeronautics and Astronautics, June 2018.
- <sup>6</sup>Falck, R. D. and Gray, J. S., "Optimal Control within the Context of Multidisciplinary Design, Analysis, and Optimization," *AIAA SciTech 2019 Forum*, No. AIAA 2019-0976 in AIAA SciTech Forum, American Institute of Aeronautics and Astronautics, January 2019.
- <sup>7</sup>Gray, J., Moore, K., and Naylor, B., "Standard Platform for Benchmarking Multidisciplinary Design Analysis and Optimization Architectures," *AIAA Journal*, Vol. 51, No. 10, October 2013, pp. 2380–2394.
- <sup>8</sup>Gray, J. S., Hearn, T. A., Moore, K. T., Hwang, J., Martins, J., and Ning, A., "Automatic Evaluation of Multidisciplinary Derivatives Using a Graph-Based Problem Formulation in OpenMDAO," *15th AIAA/ISSMO Multidisciplinary Analysis and Optimization Conference*, American Institute of Aeronautics and Astronautics, 2014/07/08 2014.
- <sup>9</sup>Chin, J. C., Schnulo, S. L., Miller, T. B., Prokopius, K., and Gray, J. S., "Battery Performance Modeling on Maxwell X-57," *AIAA SciTech 2019 Forum*, No. AIAA 2019-0784 in AIAA SciTech Forum, American Institute of Aeronautics and Astronautics, January 2019.
- <sup>10</sup>He, H., Rui, X., and Jinxin, F., "Evaluation of lithium-ion battery equivalent circuit models for state of charge estimation by an experimental approach," *Electric Vehicle Conference (IEVC)*, 4.4 582-598, Energies, March 2011.
- <sup>11</sup>Borer, N. K., Derlaga, J. M., Deere, K. A., Carter, M. B., Viken, S. A., Patterson, M. D., Litherland, B. L., and Stoll, A. M., "Comparison of Aero-Propulsive Performance Predictions for Distributed Propulsion Configurations," *AIAA SciTech 2017 Forum*, No. AIAA 2017-0209 in 55th AIAA Aerospace Sciences Meeting, American Institute of Aeronautics and Astronautics, January 2017.
- <sup>12</sup>Chin, J., Talerico, T., and Smith, A., "X-57 Modification 2 Motor Thermal Analysis," No. 2018-3410 in 2018 Flight Testing Conference, American Institute of Aeronautics and Astronautics.
- <sup>13</sup>Schnulo, S., Chin, J., and Smith, A., "Steady State Thermal Analyses of Wingtip Propulsor on SCEPTOR X-57," *17th AIAA Aviation Technology, Integration, and Operations Conference*, No. 2017-3783, American Institute of Aeronautics and Astronautics, June 2017.
- <sup>14</sup>Incropera, F. and DeWitt, D., *Fundamentals of heat and mass transfer*, J. Wiley, 2002.
- <sup>15</sup>Patterson, M. and Borer, N. K., "Approach Considerations in Aircraft with High-Lift Propeller Systems," *AIAA Aviation 2017 Forum*, No. AIAA 2017-3782 in 17th AIAA Aviation Technology, Integration, and Operations Conference, American Institute of Aeronautics and Astronautics, January 2017.